JOURNAL OF SOLID STATE CHEMISTRY 13, 32–40 (1975)

The Oxidation State of Iron in some Ba–Fe–S Phases: A Mössbauer and Electrical Resistivity Investigation of Ba_2FeS_3, $Ba_7Fe_6S_{14}$, $Ba_6Fe_8S_{15}$, $BaFe_2S_3$, and $Ba_9Fe_{16}S_{32}$

W. M. REIFF

Department of Chemistry, Northeastern University, Boston, Massachusetts 02115

I. E. GREY

Chemical Research Laboratories, Division of Mineral Chemistry, CSIRO, Port Melbourne, Victoria, Australia

A. FAN, Z. ELIEZER AND H. STEINFINK

Materials Science Laboratory, Department of Chemical Engineering, University of Texas at Austin, Austin, Texas 78712

Received February 19, 1974

Mössbauer spectroscopy, electrical resistivity, and magnetic susceptibility results are used in conjunction with crystal structure information to characterize the oxidation state of iron in five phases formed in the Ba–Fe–S system. The compounds have as a common feature FeS_4 tetrahedra which articulate by edge and corner sharing into infinite chains or columns. In Ba_2FeS_3 and $Ba_7Fe_6S_{14}$ iron is divalent in the first compound and in the latter the ratio of Fe(II)/Fe(III) is 2:1 as expected by stoichiometry. The electrons are localized and Fe(II) and Fe(III) are in definite locations in the trinuclear $[Fe_3S_6S_{2/2}]$ unit. Delocalization of electrons occurs in $Ba_6Fe_8S_{15}$, $BaFe_2S_3$, and $Ba_9Fe_{16}S_{32}$ and these compounds have low electrical resistivities and display only one quadrupole doublet in the room temperature Mössbauer spectrum. The isomer shift values of 0.2 mm/sec and 0.6 mm/sec are diagnostic of high spin Fe(III) and Fe(II), respectively, when they are in tetrahedral coordination with sulfur; intermediate values are found when electron delocalization occurs.

Introduction

We have recently described a number of barium–iron chalcogenide compounds whose three dimensional structures are based on the articulation of BaS_6 trigonal prisms. The sulfur atoms at the vertices of the prisms create tetrahedral interstices with iron filling some of them (*1*, *2*). Alternatively, the structure can be described in terms of FeS_4 tetrahedra which link by edge and/or corner sharing into infinite chains or columns which are separated by about 6 Å from adjacent units and these columns in turn are linked laterally by barium ions located in the centers of trigonal prisms formed by the sulfur atoms of the chains. For an understanding of the physical properties of these compounds the infinite linear chain description is advantageous because it emphasizes the one dimensional array of iron–iron and sulfur–iron interactions. Figures 1 and 2 show schematic outlines of the tetrahedral structural units for the compounds investigated. Infinite linear chains of FeS_4 tetrahedra sharing corners are present in Ba_2FeS_3; columns of edge shared tetrahedra exist in $Ba_9Fe_{16}S_{32}$;

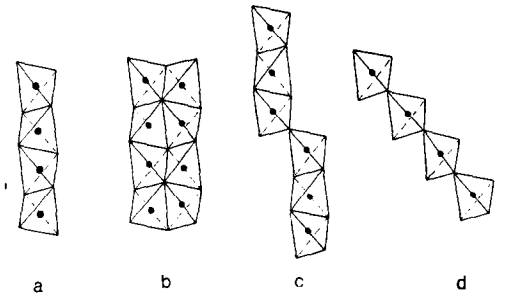

FIG. 1. The articulation of FeS_4 tetrahedra in (a) $Ba_9Fe_{16}S_{32}$, (b) $BaFe_2S_3$, (c) $Ba_7Fe_6S_{14}$, and (d) Ba_2FeS_3.

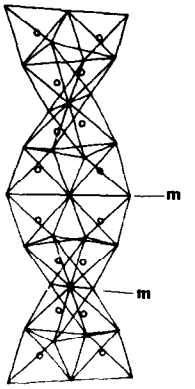

FIG. 2. The columnar chain of FeS_4 tetrahedra in $Ba_6Fe_8S_{15}$. The four corner sharing tetrahedra are between the lines indicating the mirror planes, *m*, and propagation along the *c* axis occurs by reflection.

zigzag linear chains of tetrahedra are found in $Ba_7Fe_6S_{14}$; infinite double chains in $BaFe_2S_3$; and a columnar-type structure is present in $Ba_6Fe_8S_{15}$. The structural information shows that sulfur must be considered as a divalent anion so that several of the stoichiometries require the presence of mixed oxidation states for iron. Two models are possible for such mixed valence states, i.e., the electrons are localized or fast exchange occurs and one observes an averaged value. In the former case the additional complication of static disorder of Fe(II) and Fe(III) in crystallographic sites is possible. For stoichiometries that formally require only a single oxidation state delocalization can also occur and thus influence the physical properties.

Previous studies of mixed oxidation state iron compounds have involved interesting but structurally different examples such as orthorhombic cubanite $CuFe_2S_3$ (*3*), greigite Fe_3S_4 (*4*, *5*), magnetite Fe_3O_4 (*6*), and pyrrhotite Fe_7S_8 (*7*, *8*). In this investigation we examine the electrical and magnetic behavior and Mössbauer spectra of a series of structurally related compounds with the expectation that the underlying connection between structure and physical properties will emerge.

Experimental

Mössbauer spectra were obtained using a constant acceleration drive operated in the time mode. Data were accumulated in a Northern Scientific Co. 512 channel analyzer. The source was 50 mC; of ^{57}Co diffused into copper foil and used at room temperature. All isomer shifts are with respect to 99.99% iron foil. The absorbers consisted of finely ground powder of thickness ≈ 5 mg natural iron/cm^2. The spectra were fitted by least-squares analysis assuming lorentzian line shapes and using a modified National Bureau of Standards program (*9*). The reproducibility for values of isomer shifts and quadrupole splittings is ± 0.02 mm/sec.

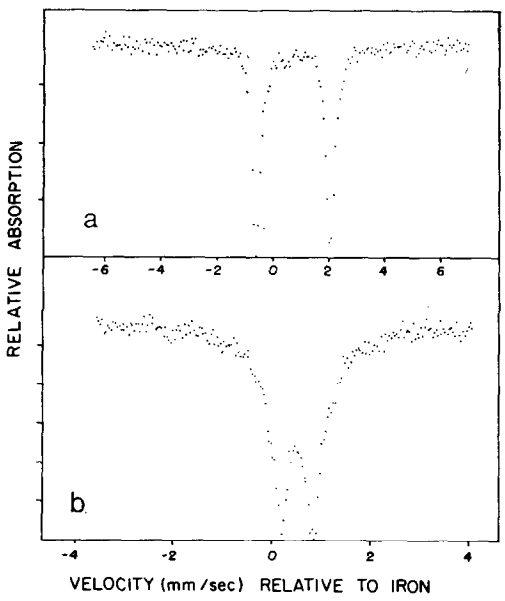

FIG. 3. (a) Mössbauer spectrum of Ba_2FeS_3 at 78 K. (b) Mössbauer spectrum of $BaFe_2S_3$ at 78 K.

Electrical resistivity measurements were carried out on pressed and sintered samples and for $BaFe_2S_3$ data were also obtained on a single crystal. The sintered samples were obtained by applying a pressure of about 10 000 psi to a finely powdered specimen and then heating it in vacuum at 500°C for about two days. The measurements were made using either a milliohmmeter or an electrometer depending on the resistivity. A conventional four-probe method was used for the rectangular shaped pressed samples and for irregularly shaped specimens the van der Pauw (*10*) method was employed. The high temperature measurements were made in a protective atmosphere of argon. The measurements of magnetic susceptibility as a function of temperature were carried out on a Faraday balance. From plots of $1/x$ vs T the magnetic moments and θ temperatures were deter-

TABLE I

MÖSSBAUER PARAMETERS (mm/sec)[a]

Compound	Temperature (°K)	δ	ΔE	H(kG)	Reference
1. Ba_2FeS_3	300	0.62	2.56		[b]
	78	0.75	2.64		
2. Ba_2FeSe_3	300	0.66	2.56		[b]
	78	0.76	2.72		
3. $FeCr_2S_4$	295	0.60	0		(*3*)
4. Cu_2FeSnS_4	295	0.57	2.90		(*3*)
5. $FeIn_2S_4$	295	0.88	3.27		(*3*)
6. $Fe[SP(CH_3)_2NP(CH_3)_2S]_2$	300	0.67	3.17		[b]
		0.79	3.34		
7. $Ba_9Fe_{16}S_{32}$	300	0.20	0.65		
	195	Partially ordered			
	78			229 248	[b]
8. $KFeS_2$	300	0.16	0.52		
	128			206	(*3, 23*)
9. $CuFeS_2$	300	0.23	0.49	356	(*3*)
	78	0.37	0.63	368	
10. $Ba_7Fe_6S_{14}$	300	0.17 (1–4)	1.13		[b]
		0.39 (2–5)	1.46		
		0.66 (3–6)	1.33		
	195				
	78			243 263 295	
11. $CuFe_2S_3$	300	0.39		322	(*3*)
	78	0.52		339	
12. $Ba_6Fe_8S_{15}$	300	0.47	0.68		[b]
	195	0.54	0.71		
	78			156 177	
13. $BaFe_2S_3$	300	0.41	0.60		[b]
	78	0.53	0.67		
14. $BaFe_2Se_3$	300	0.47	0.71		[b]

[a] Relative to Fe foil.
[b] This work.

mined. The possible influence of ferromagnetic impurities on the susceptibility data was eliminated by the method of Honda and Owen (*11*).

Results

Ba_2FeS_3

The structure consists of infinite linear chains of identical corner sharing tetrahedra and stoichiometry implies the presence of ferrous iron only. The single large quadrupole, (Fig. 3a), indicates that the iron atoms are equivalent although in a distorted environment, Ba_2FeSe_3 is isomorphous with the sulfide and its Mössbauer parameters are rather similar to it (Table I). The isomer shifts of compounds 1 and 2 should be compared to those of 3, 4, and 5 in Table I. Compound 3, a normal spinel (*12, 13*), and 4 (*14*), contain arrays of $Fe(II)S_4$ tetrahedra while 5, an inverse spinel (*15*), contains $Fe(II)S_6$ octahedra. The smaller isomer shifts observed for the four coordinate systems are consistent with the usual systematics of variations for ^{57}Fe isomer shifts with coordination number (*16, 17*). We have also determined the Mössbauer spectrum of Bis[(imidotetramethyldithiophosphino)-S, S] iron II, $[SP(CH_3)_2(NPCH_3)_2S]_2Fe$, compound 6 in Table I. Previous (*18*) magnetic and spectral studies have shown that this compound contains high-spin ferrous ion tetrahedrally coordinated by four sulfur atoms. The latter has recently been confirmed (*19*) in an X-ray investigation that shows the complex to be a tetrahedral FeS_4 monomer with some distortion of the coordination environment. The isomer shift, δ, for this compound is quite similar to that of compounds 1 and 2 and we therefore propose a value of 0.6 mm/sec as diagnostic of the tetrahedral ferrous ion coordinated to sulfur.

The temperature dependence of the Mössbauer spectrum of Ba_2FeS_3 is also consistent with a high-spin ferrous ion in that no Zeeman splitting is observed for its spectrum at 78 K, although magnetic data show that the material is antiferromagnetically ordered below about 110 K (*20*). Rapid spin-lattice relaxation in ferrous systems may result in Zeeman splitting of Mössbauer spectra at temperatures somewhat lower than ordering temperatures determined by bulk susceptibility measurements. For the more "ferric" like systems discussed below, where spin–spin relaxation is usually the predominant relaxation mechanism, low temperature Zeeman splitting is more readily observed.

The indication that Fe(II) is present in Ba_2FeS_3 is further confirmed by the measured magnetic moment, Table II. The theoretical effective magnetic moments for Fe(II) and Fe(III) are 4.9 and 5.9 μ_B, respectively, and intermediate values are to be expected for mixed valence states. The measured magnetic moment by itself cannot determine whether mobile electrons (delocalized) are present. The isomer shift will similarly not distinguish between mobile electrons or a static disorder of Fe(II) and Fe(III) in crystallographic sites. However, the electrical resistivity is expected to be relatively high when localized electrons are present and should be relatively

TABLE II

SUMMARY OF PARAMAGNETIC MOMENT, ROOM TEMPERATURE ELECTRICAL RESISTIVITY, AND BAND GAP

Compound	Effective moment (μ_B)	Room temperature electrical resistivity (ohm cm)	Activation energy E (eV)	Room temperature Seebeck coefficient (μV/K)
Ba_2FeS_3	5.29	10^4	0.60	—
$Ba_7Fe_6S_{14}$	5.70	10^3	0.62	—
$BaFe_2S_3$	4.85	0.5	0.16	−33.0
$Ba_6Fe_8S_{15}$	5.57	1.0	0.31	−25.0
$Ba_9Fe_{16}S_{32}$		1.0	0.14	

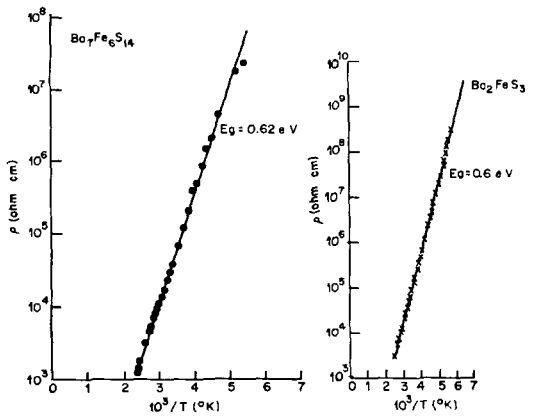

FIG. 4. The electrical resistivity vs $1/T$ for $Ba_7Fe_6S_{14}$ and Ba_2FeS_3.

low when fast electron exchange, i.e., mobile electrons, are present. The magnetic moment, the isomer shift and the high electrical resistivity (Fig. 4) are consistent with Fe(II) in agreement with the valence expected from the stoichiometry.

$Ba_7Fe_6S_{14}$

The structure consists of infinite linear zigzag chains formed by trinculear units composed of a central tetrahedron sharing two edges with two adjacent tetrahedra. The outside tetrahedra share corners with other trinuclear units to form the chain, Fig. 1. The magnetic moment (Table II) (*20*), is consistent with an averaged value for the iron oxidation states expected on the basis of stoichiometry. We interpret the high electrical resistivity (Fig. 4), as due to localized electrons on the crystallographic iron sites. The environment of the three iron atoms in the basic trinuclear unit (Fig. 5) (*2*) differs slightly

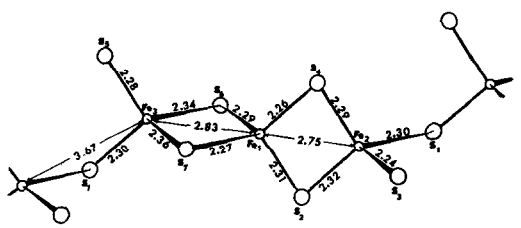

FIG. 5. Bond lengths for the trinuclear unit $[Fe_3S_6S_{2/2}]$ in $Ba_7Fe_6S_{14}$.

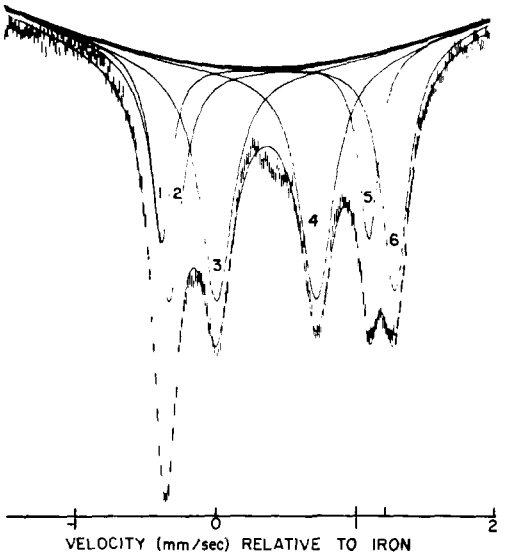

FIG. 6. Room temperature Mössbauer spectrum of $Ba_7Fe_6S_{14}$. The three quadrupole doublets are 1–4, 2–5, 3–6.

and three sets of quadrupole split lines are observed at room temperature. The matching of the lines shown in Fig. 6, 1–4, 2–5, and 3–6 yields the parameters shown in Table I. The first doublet represents Fe(III) and the third pair yields an isomer shift indicative of Fe(II); the intermediate value of 0.39 mm/sec is difficult to understand. The calculated areas from the fit are in the ratio 1 : 2 in excellent agreement with expectation from the stoichiometry of the compound. Another interpretation of the Mössbauer data results if the quadrupole doublets are matched by the association of lines 1–6, 2–5, and 3–4 which yield isomer shifts of 0.49, 0.36, and 0.36, respectively. This analysis implies the presence of delocalized electrons. The high electrical resistivity, however, indicates that the delocalization is restricted to the trinuclear unit. The 3.67 Å distance between Fe–Fe located in the tetrahedral interstices of the corner-sharing tetrahedra prevents the overlap of orbitals between the units, and no continuous conduction band is formed. This explanation is preferable because it accounts unambiguously for the three intermediate values of isomer shift.

With a Néel temperature of about 200 K (*20*) $Ba_7Fe_6S_{14}$ orders antiferromagnetically.

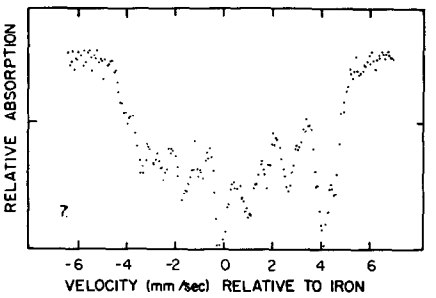

FIG. 7. Mössbauer spectrum of $Ba_7Fe_6S_{14}$ at 78 K.

At 195 K the spectrum of $Ba_7Fe_6S_{14}$ is identical to that at room temperature, i.e., not magnetically split, again reflecting the difference in time scales between Mössbauer spectroscopy and bulk susceptibility measurement with respect to the observation of ordering phenomena. At 78 K the magnetic ordering is clearly reflected in a very complicated spectrum (Fig. 7) whose most reasonable interpretation is that it results from the overlap of three 6-line Zeeman patterns corresponding to the three room temperature quadrupoles. The internal fields vary from 240 to 295 kG indicating a fair degree of covalency as compared to, e.g., tetrahedral halides and oxides.

$Ba_6Fe_8S_{15}$

The fundamental structural unit is an infinite columnar arrangement of FeS_4 tetrahedra (Fig. 2), and the magnetic moment is consistent with the average expected for 2 Fe(III) and 6 Fe(II) on the basis of the stoichiometry. The electrical resistivity (Fig. 8) is quite low indicative of mobile electrons. Thus, all the iron atoms are expected to be equivalent and indeed only a single quadrupole doublet is observed in the Mössbauer spectra obtained at 300 and 195 K, Fig. 9a. An intermediate value for the isomer shift is observed (Table I), and we conclude that the oxidation state of iron has an average value of about 2.25.

The low temperature magnetic ordering of $Ba_6Fe_8S_{15}$ is observed in the Zeeman spectrum of Fig. 9b where two overlapping hyperfine patterns of equal intensity are indicated by the stick diagrams. The hyperfine fields are

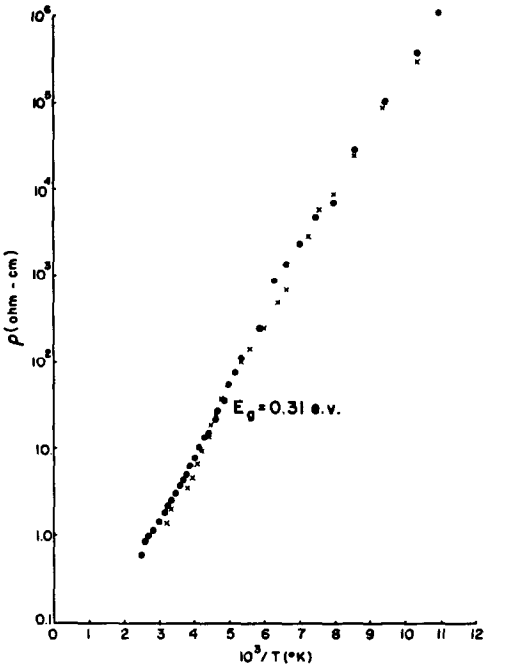

FIG. 8. The electrical resistivity vs $1/T$ for $Ba_6Fe_8S_{15}$. × cool down, ● warm up.

small and most probably correspond to considerable covalency and delocalization. The presence of two hyperfine fields suggests

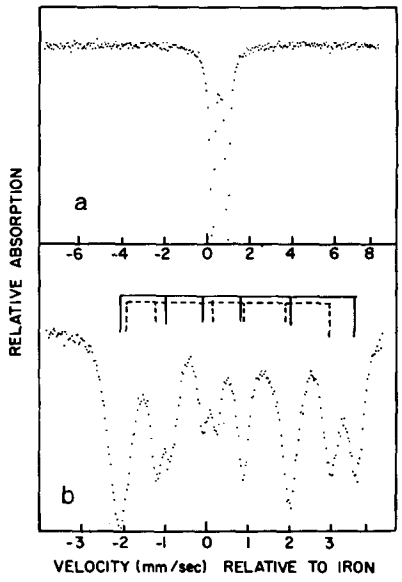

FIG. 9. The Mössbauer spectrum of $Ba_6Fe_8S_{15}$ at (a) 300 K and (b) 78 K.

site inequivalency contrary to the higher temperature Mössbauer and X-ray results. Possibly this inequivalency is induced by a low temperature phase transition, crystallographic or more likely, magnetic rather than cation ordering (Verwey type transition). In the latter circumstances, two hyperfine patterns corresponding to Fe(II) and Fe(III) in the ratio of 3:1 might be expected.

$BaFe_2S_3$

The structure consists of infinite linear double chains (Fig. 1) and Fe(II) is indicated by the stoichiometry. Resistivity measurements on single crystals and polycrystalline bars (Fig. 10) show a rather low resistivity. The magnetic susceptibility data yield a moment consistent with divalent iron (Table II), and this material is paramagnetic. The Mössbauer spectrum (Fig. 3b) shows only a single quadrupole with an intermediate value of the isomer shift between di- and trivalent iron. The spread of the bond angles and bond distances for this phase leads to the expectation of a somewhat smaller quadrupole than for Ba_2FeS_3 and this is the case. Similar structural and Mössbauer parameters are observed for the selenium analogue. No relaxation broadening or Zeeman splitting is observed at 78 K consistent with paramagnetic behavior. The isomer shift is almost exactly intermediate between the extremes we have suggested for ferrous and ferric iron and delocalization occurs to the extent of nearly one half electron per iron.

$Ba_9Fe_{16}S_{32}$

The preliminary results of a structural investigation indicate that an infinite linear chain of edge sharing tetrahedra (Fig. 1) similar to that of $KFeS_2$ (*21*) is present. In fact all of its Mössbauer parameters such as isomer shift, quadrupole splitting, and average internal hyperfine field, are very similar to those of $KFeS_2$ (*3*, *22*) and to chalcopyrite, $CuFeS_2$, a mineral containing tetrahedral (*24*, *25*) high-spin Fe(III). Isomer shifts of about 0.20 mm/sec and small quadrupole splittings seem to be diagnostic of high-spin Fe(III). The stoichiometry of $Ba_9Fe_{16}S_{32}$

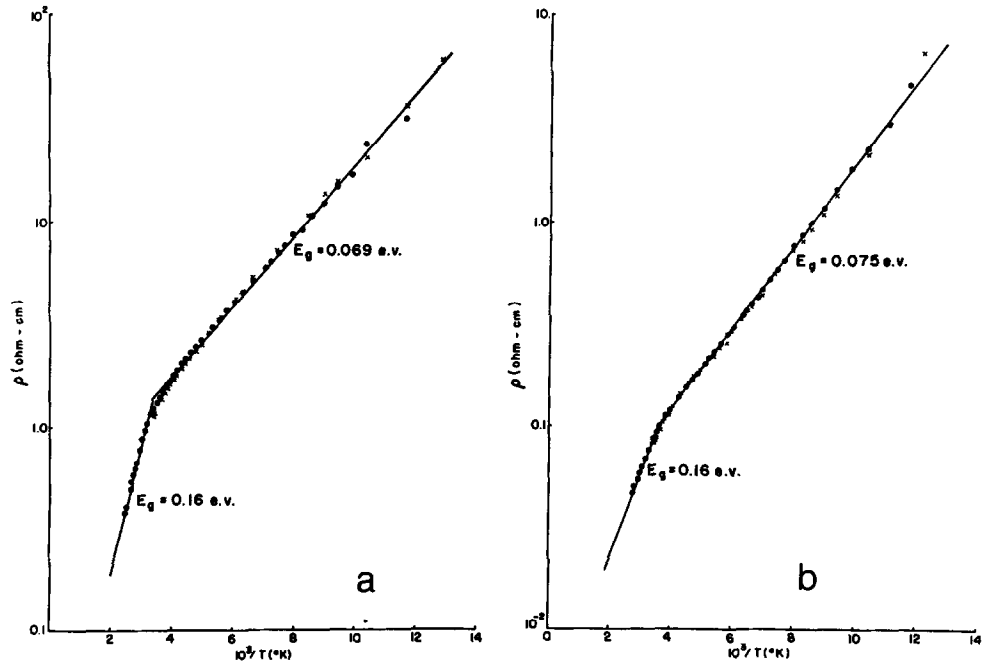

FIG. 10. Electrical resistivity of $BaFe_2S_3$ single crystal (a) perpendicular to the *c* axis and (b) parallel to the *c* axis.

suggests the mixed oxidation system $Ba[Fe_{14}(III)Fe_2(II)]S_{32}$ and an average oxidation state of 2.88 i.e., weighted toward 3 in the event rapid electron transfer occurs between Fe(II) and Fe(III) centers. The latter situation is consistent with the observed single quadrupole and value of the isomer shift for the room temperature spectrum (Fig. 11a).

At 78 K the spectral behavior is more complicated (Fig. 11b) in that there is now overlap of two and possibly three hyperfine patterns whose fields are similar to those for $KFeS_2$ (*22*). The intensities of the overlapping hyperfine patterns appear to be about the same and a cation ordering, a so-called Verwey transition (*25*), to localized iron oxidation states is not suggested. For such an occurrence one might expect to see two hyperfine patterns whose areas are in the ratio of 7:1 in accord with the stoichiometry. Possibly magnetic ordering or, less likely, a low temperature crystallographic phase transition causes site inequivalency. The resisitivity of this material is of the same magnitude as for $Ba_6Fe_8S_{15}$ and $BaFe_2S_3$, indicative of mobile electrons.

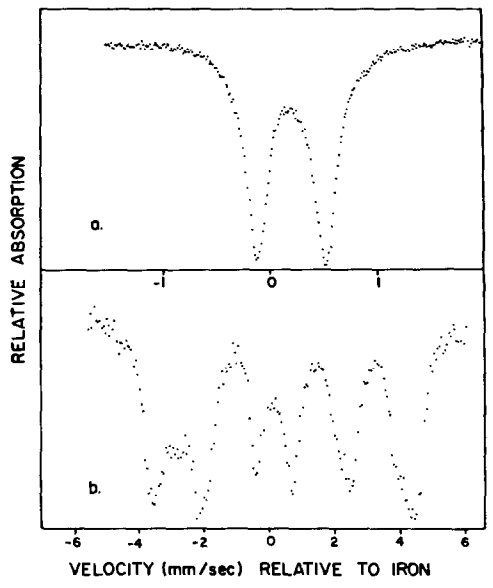

FIG. 11. Mössbauer spectra of $Ba_9Fe_{16}S_{32}$ at (a) room temperature, (b) 78 K.

Conclusion

The compounds discussed in this investigation have structures based on the articulation of FeS_4 tetrahedra by edge or corner sharing or by both. The Mössbauer isomer shifts for high-spin divalent and trivalent iron tetrahedrally coordinated to sulfur in these compounds and in previously investigated compounds listed in Table I lead us to suggest that 0.60 mm/sec and about 0.20 mm/sec, respectively, can be considered diagnostic values for these oxidation states. It is evident that an intermediate value of the isomer shift can indicate electron delocalization but must be confirmed by electrical measurements.

A survey of Fe–S bond lengths shows that conclusions about the oxidation state of iron based on such values are not possible. In Ba_2FeS_3, where only high spin Fe(II) is present, the Fe–S length is 2.45 Å when S is shared between two Fe ions and the other distances are 2.30 and 2.38 Å. Generally distances are about 2.3 Å with variations of about ± 0.1 Å in the same tetrahedron because of different environments of the S atoms. No systematic variation in the Fe–S bond length occurs as a function of high-spin or low-spin iron or as a function of the mobility of the 3*d* electrons. Magnetic data are required to indicate the spin state of Fe, Mössbauer isomer shifts will show the oxidation state but cannot distinguish between an averaged value due to mobile electrons or due to a static, crystallographically disordered distribution of di- and trivalent iron. Values of the electrical resistivity can then be very helpful in deciding which of the two possibilities exist.

Acknowledgments

W. M. Reiff is grateful for the support of the Research Corporation, the donors of the Petroleum Research Fund and the National Science Foundation (Grant No. 39010). He also thanks Dr. A. Davison and co-workers for the sample of compound No. 6 (Table I). The other authors acknowledge the research support by the Air Force Office of Scientific Research, Office of Aerospace Research, United States Air Force under AFOSR Grant No. 72-2199 and the Robert A. Welch Foundation, Houston, Texas.

References

1. H. Hong and H. Steinfink, *J. Solid State Chem.* **5**, 93 (1972).
2. I. E. Grey, H. Hong, and H. Steinfink, *Inorg. Chem.* **10**, 340 (1971).
3. N. N. Greenwood and H. J. Whitfield, *J. Chem. Soc. A*, 1697 (1968).
4. J. M. D. Coey, M. R. Spender, and A. H. Morrish, *Solid State Commun.* **8**, 1605 (1970).
5. D. J. Vaughan and M. S. Ridout, *J. Inorg. Nucl. Chem.* **33**, 741 (1971).
6. R. S. Hargrove and W. Kundig, *Solid State Commun.* **8**, 303 (1970).
7. L. M. Levinson and D. J. Treves, *J. Phys. Chem. Solids* **29**, 2227 (1968).
8. D. J. Vaughan and M. S. Ridout, *Solid State Commun.* **8**, 2165 (1970).
9. E. Rhodes, W. O'Neal, and J. J. Spijkerman, *Nat. Bur. Std. Tech. Note* **404**, 108 (1966).
10. L. J. van der Pauw, *Philips Res. Rept.* **13**, 1 (1958).
11. L. F. Bates, "Modern Magnetism," 4th Ed. p. 134. Cambridge University Press, 1963.
12. H. Hahn, *Z. Anorg. Chem.* **264**, 184 (1951).
13. F. K. Lotgering, *Philips Res. Rept.* **11**, 337 (1956).
14. L. O. Brockway, *Z. Kristallogr.* **89**, 434 (1934).
15. H. Hahn and W. Klinger, *Z. Anorg. Chem.* **263**, 177 (1950).
16. N. E. Erickson, "Advances in Chemistry Series," No. 68, 86. American Chemical Society, Washington, D.C., 1967.
17. P. R. Edwards and C. E. Johnson, *J. Chem. Phys.* **47**, 2074 (1967).
18. A. Davison and E. S. Switkes, *Inorg. Chem.* **10**, 837 (1971).
19. M. R. Churchill and J. Wormald, *Inorg. Chem.* **10**, 1778 (1971).
20. H. Steinfink, H. Hong, and I. E. Grey, *National Bureau of Standards Special Publication* **364**, *Proceedings of 5th Materials Research Symposium*, 681 (1972).
21. J. W. Boon and C. H. MacGillavry, *Rec. Trav. Chim.* **61**, 910 (1942).
22. E. Fluck, W. Kerler, and W. Neuwirth, *Angew. Chem. Int. Ed.* **2**, 277 (1967).
23. L. Pauling and L. D. Brockway, *Z. Krist.* **82**, 188 (1932).
24. J. W. Boon, *Rec. Trav. Chim.* **63**, 69 (1944).
25. E. J. W. Verwey, *Nature (London)* **144**, 327 (1939).